Results

Investigating the role of transport receptors in Ran induced microtubule assembly

Previous work had shown that Ran induces microtubule assembly in *Xenopus laevis* M-phase extracts. One possibility for Ran to function in this process was by acting the same way it does in nucleocytoplasmic transport during interphase by one of its two possible mechanisms. Either RanGTP recruits an export receptor, or RanGTP dissociates an import receptor from a cargo molecule. In the latter case the import receptor would serve as an inhibitor for the cargo molecule in its function to assemble microtubules.

The import adaptor importin α is mostly bound to NLS-cargo molecules as well as to importin β in *Xenopus* extracts (Gorlich *et al*., 1995a). Dissociating importin β from a trimeric complex of NLS-cargo importin α/β reduces the affinity of importin α for an NLS-cargo (Rexach and Blobel, 1995). Replacing importin β by adding the importin β binding domain from importin α, IBB, should therefore free the cargo and lead to microtubule assembly. Similarly, addition of excess NLS cargo molecules should displace importin α from NLS cargo and also lead to microtubule assembly. Microtubule assembly was tested by adding rhodamine labeled tubulin to M-phase *Xenopus* extracts and incubating for 30 min at room temperature. Samples were fixed by the addition of 6 % formaldehyde and covered with a glass slide. Images where taken on a confocal microscope and asters counted in a given field. In this experiment 50 µM IBB did cause microtubule assembly (Figure 8) while a truncated form of IBB, which had been shown to be deficient in interacting with importin β (Gorlich *et al*., 1996a), did not show aster formation, indicating that this effect is specific.

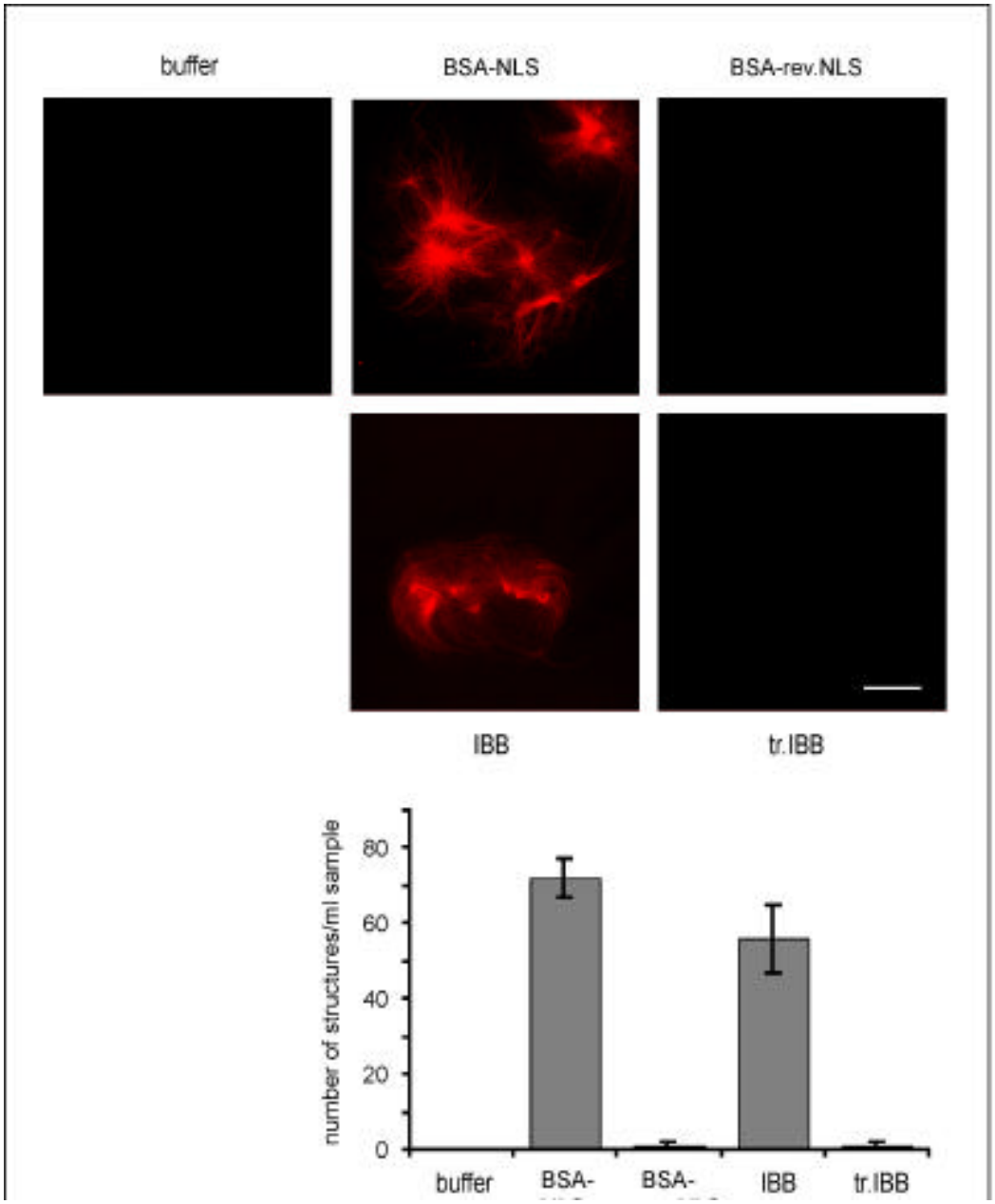

Figure 8. NLS-peptide induces aster formation in *Xenopus* M-phase extract. Microtubule assembly was tested in M-phase *Xenopus* egg extracts in the presence of rhodamine-labeled tubulin for 30 min after preincubation with either buffer, 30 µM NLS peptide coupled to BSA (BSA-NLS), or a nonfunctional reverse NLS peptide (BSArev.NLS), (upper panels) and after preincubation with 50 µM IBB or truncated IBB (tr. IBB), (lower panels). Scale bar 20 µm. Histogram: Results were quantified by counting structures from six fixed and squashed samples. Error bars represent standard deviations.

Moreover 30 µM NLS peptide coupled to BSA induced microtubule nucleation in *Xenopus* mitotic extract. Addition of reverse NLS coupled to BSA had no effect indicating that the nucleation by BSA-NLS is specific (Figure 8). This experiment

suggested that an NLS containing cargo exists, which is bound by importin α and thus inactive in nucleating microtubules. Competition with IBB, BSA-NLS or addition of RanGTP would release the NLS containing factor from its inhibitor, importin α, and the factor would then be free to nucleate microtubules.

This predicts that importin α binds to the Ran regulated nucleators by an NLS and that a large concentration of importin α could inhibit RanGTP mediated microtubule assembly. To test for this possible regulation of Ran-induced microtubule assembly by importin α we set out to design importin α mutants which do not bind NLS containing proteins, to be able to distinguish specific from unspecific effects. The crystal structure of yeast importin α bound to either c-myc NLS peptide or nucleoplasmin NLS peptides revealed two independent binding sites, a large and a small one. The large binding site forms specific interactions with five lysine or arginine residues from the NLS peptide which is thought to be crucial for the binding of monopartite NLS peptides. Bipartite NLS peptides are bound to both binding pockets at the same time. The structure predicted aspartic acid 203 in the large binding pocket and glutamic acid 402 in the small binding pocket to be critical for electrostatic interactions with the positive charged NLS peptide (Conti and Kuriyan, 2000; Conti *et al*., 1998). In order to create a mutant version of importin α, which can no longer bind NLS sequences we took the *Xenopus* importin α gene and changed D189 and E389 into lysine and arginine individually using PCR directed mutagenesis. We subsequently cloned a double mutant version where both sites are changed into basic amino acids. Recombinant proteins were prepared from these constructs and assayed for binding to nucleoplasmin, a protein containing a bipartite NLS sequence (Figure 9).

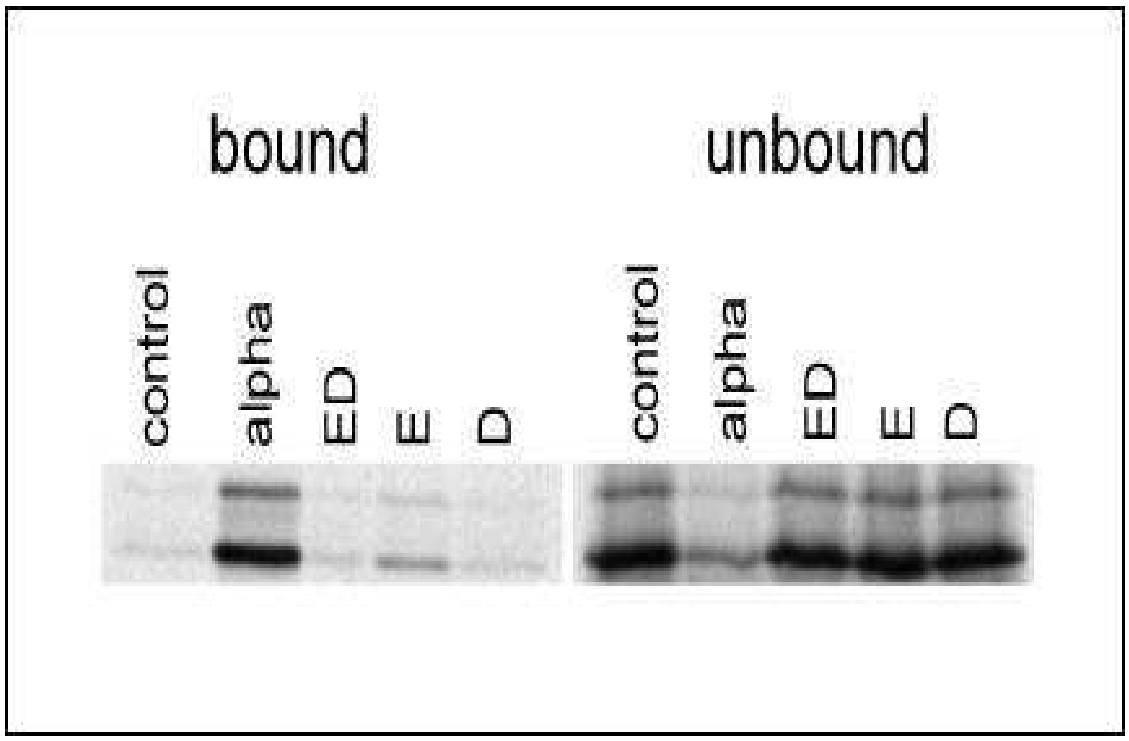

Figure 9. A mutation of importin α is unable to bind to an NLS protein. *In vitro* translated, ^{35}S-methionine-labeled nucleoplasmin was incubated with protein A-tagged importin α or importin α containing point mutations in the NLS binding pockets bound to IgG sepharose. Empty beads served as a further control. Nucleoplasmin binding was analyzed by SDS-PAGE and autoradiography.

Wild type recombinant importin α protein wild type and mutant versions were immobilized on a column and *in vitro* translated, radioactively labeled nucleoplasmin was passed over the column and assayed for binding by SDS-PAGE and autoradiography (Figure 9). Nucleoplasmin protein bound to importin α wild type but not to empty beads as a control (Figure 9 lanes 1 and 2). A double mutant of importin α in which both D189 and E389 were mutated, as well as the D189 single mutant, were severely affected in binding to a bipartite NLS protein (Figure 9 lanes 3 and 5). A mutation at the E389 site also had a considerable effect, but did not disrupt binding of importin α to nucleoplasmin completely (Figure 9 lane 4). This data reconfirms the idea (Conti and Kuriyan, 2000) that the large binding pocket, with the D189 site, is most critical for bipartite NLS binding.

Importin α is exported from the nucleus in a trimeric complex with RanGTP and CAS. The binding site for CAS lies at the C-terminus of the protein between amino acids 383-497 including arm repeats seven and eight and the acidic domain (Herold *et al*., 1998). To test whether the generated importin α mutants are active in binding independent from the NLS binding pockets and to further characterize the mutants we assayed them for their ability to bind to their export receptor CAS (Figure 10). Protein A tagged importin α or mutant protein was immobilized on an IgG column and CAS and RanGTP together were passed over the column.

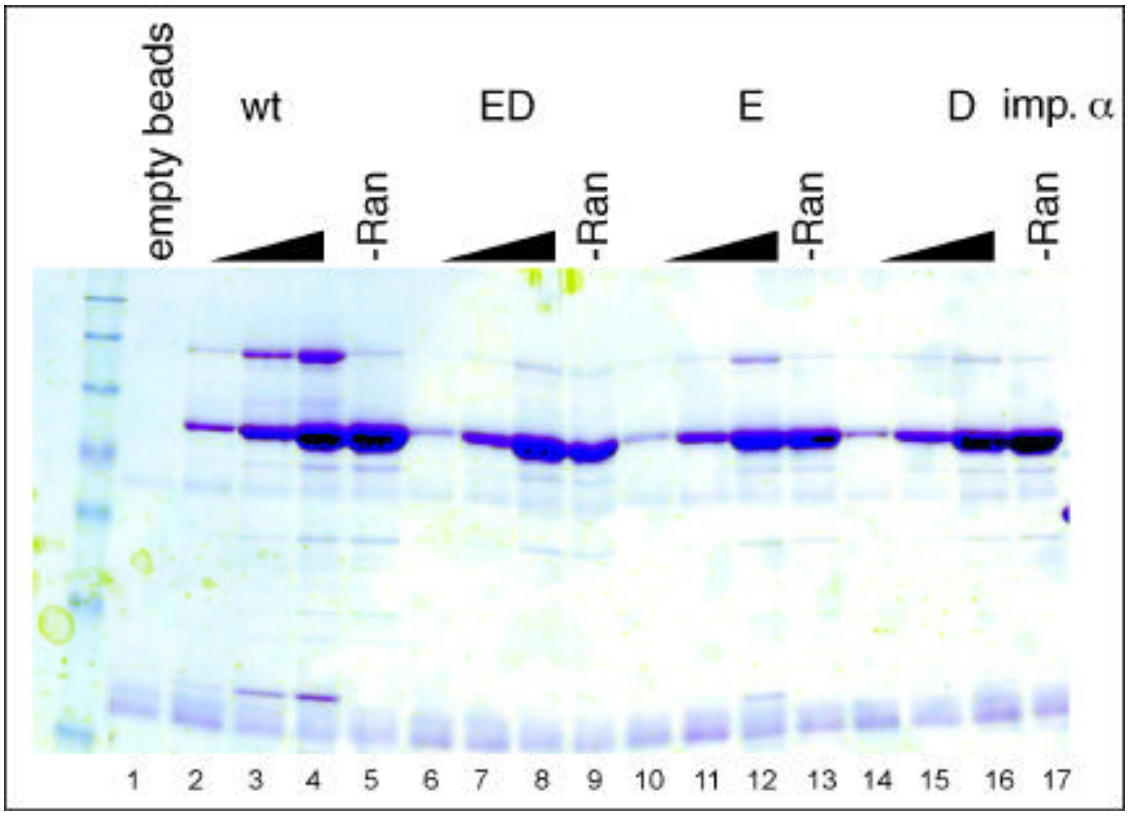

Figure 10. Point mutations in importin α affect CAS binding. Increasing amounts of importin α or point mutant proteins were immobilized on IgG sepharose and RanQ69LGTP and CAS were assayed for binding by SDS-PAGE. Empty beads on the left and lanes with no Ran to the right serve as controls.

Binding of CAS and RanGTP to importin α was assayed by SDS-PAGE and Coomassie blue staining. Wild type importin α bound CAS in a RanGTP

dependent manner (Figure 10). There was some binding of all three mutants to CAS but while the E389R single mutant showed stronger binding to CAS both the single point mutant D189K and the double mutant E389R D189K were severely affected in CAS binding. It was shown that NLS peptides and CAS can not bind to importin α simultaneously even although their binding sites do not overlap suggesting a conformational change of importin α upon NLS cargo binding (Herold *et al*., 1998). Since a mutation at D189, far away from the CAS binding site between 383-497, affects CAS binding D189K might affect this conformational change in importin α.

Ran induces MT assembly by reversing the inhibition by importin α

The importin α mutants could now be used as a tool to distinguish specific effects of importin α due to its ability to bind NLS proteins from unspecific effects. Since RanGTP, BSA-NLS and IBB, which all disassemble import complexes, induced aster formation in *Xenopus* M-phase extract importin α was possibly counteracting these factors by forming an import complex. We wanted to find out if importin α inhibits aster formation by binding to an NLS-cargo. *Xenopus* mitotic extracts were prepared and pre-incubated with either buffer or importin α wild type or mutants for 45 min on ice to allow complexes to form (Figure 11). Then asters were induced by adding 7.5 µM of RanQ69LGTP, a mutant Ran protein defective in GTP hydrolysis (Bischoff *et al*., 1994), to the samples. After 25 min incubation at 25°C 1.5 µl of the reaction was dropped on a cover slip, squash fixed and pictures taken on a confocal microscope (Figure 11).

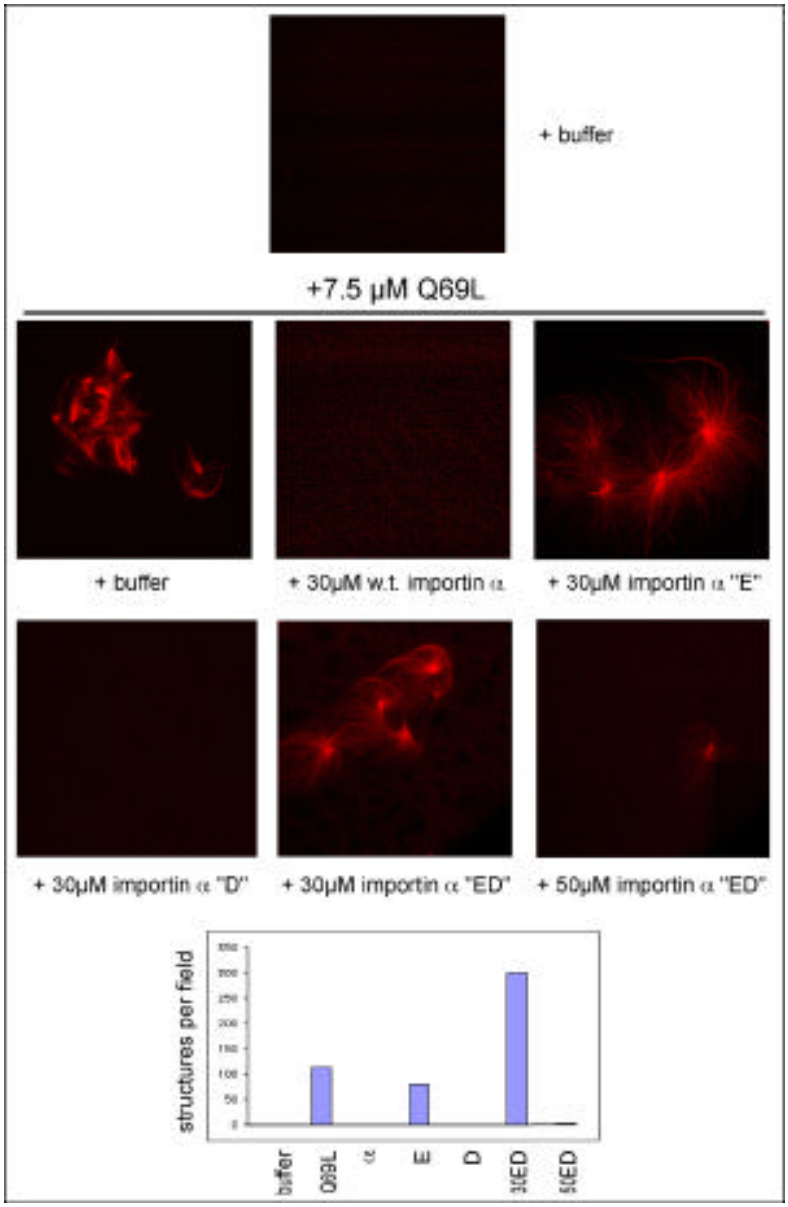

Figure 11. Importin α acts to inhibit microtubule assembly in egg extract. Microtubule assembly was tested in egg extracts incubated for 20 min with (top panel) or without the addition of 7.5 µM RanQ69LGTP and with importin α or the point mutants E, D or ED at 30 µM or 50 µM together with RanQ69LGTP. Scale bar 20 µm. Histogram: Results were quantified by counting structures in a field.

Aster formation induced by RanQ69LGTP was inhibited by 30 µM importin α as well as by 30 µM importin α "D" (Figure 11). The "E" and "ED" mutations did not inhibit aster formation at this concentration but also reduced the amount of asters

at higher concentrations (Figure 11). This indicates that importin α specifically inhibits Ran induced microtubule assembly due to its ability to bind NLS-cargos. Since the "E" mutation, which still binds nucleoplasmin to some extent, does not inhibit aster formation, the experiment above suggested that the putative importin α cargo likely contains a monopartite NLS sequence. The fact that a high concentration of the "ED" mutant protein can inhibit microtubule formation may either reflect non-specific effects or the retention of a very weak affinity for NLSs in the mutant.

Purification of the Ran dependent nucleation activity

The ability of importin α to inhibit aster formation suggested a method to deplete the nucleation factors from egg extracts. Both RanQ69LGTP and a large excess of importin α carrying the z domain of *Staphylococcus aureus* protein A were added to *Xenopus* egg extract. RanGTP induces dissociation of proteins bound to endogenous importin α via its interaction with importin β and CAS. These proteins will mainly rebind to the exogenous importin α when it is added in excess, and can then be removed with an IgG column. Using the "ED" mutation as a control we were able to distinguish between proteins which bind unspecifically to importin α from those which bind through their NLS sequence to importin α (Figure 12). Depleting egg extracts with an importin α column depleted the aster forming activity, depleting extracts using the "ED" control did not deplete the activity (Figure 12).

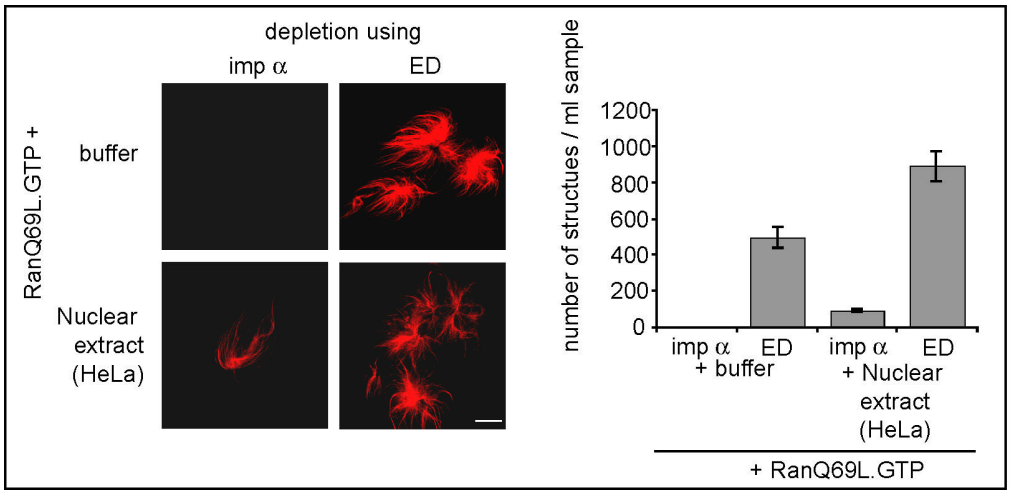

Figure 12. HeLa nuclear extract restores the activity of extracts depleted of NLS proteins. Microtubule assembly was tested in extracts depleted with importin α (imp α) or the ED mutant by incubating extracts for 20 min. To restore the activity depleted extracts were supplemented with either 1/10 volume of HeLa nuclear extract or buffer as a control. Scale bar 20 nm. Results were quantified by counting structures in a field. Error bars represent standard deviations.

Next, we tried to restore the activity in extracts depleted using immobilized importin α. Different sources of NLS proteins were tested. Restoration was possible by adding back either HeLa cell nuclear extract or a fraction of proteins precipitated by addition of 20% ammonium sulfate to *Xenopus laevis* extract (Figure 12). Oliver Gruss fractionated HeLa nuclear extract by ammonium sulphate cuts, fractions were assayed for nucleating activity by adding them to *Xenopus* extracts depleted of NLS-proteins and inactive in aster formation (Figure 13).

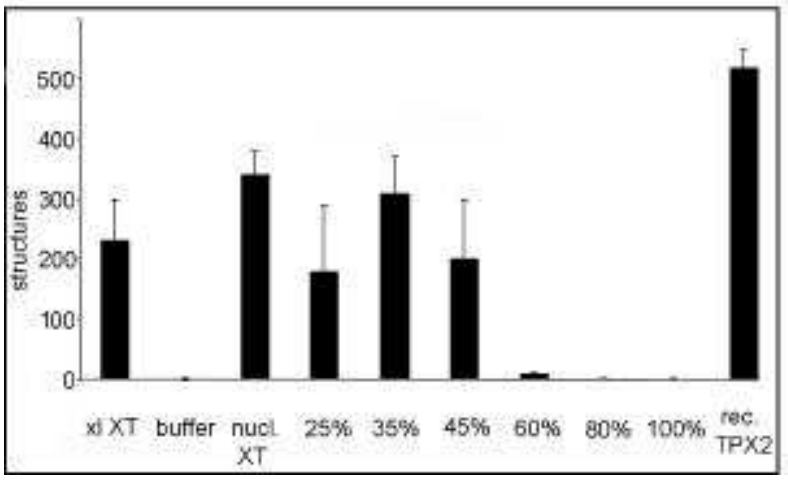

Figure 13. Activity of egg extract depleted of NLS proteins can be restored with fractionated extract. Egg extract was depleted with importin α and reactivated with 1/10 volume Xenopus egg extract, HeLa nuclear extract, ammonium sulphate fractions of nuclear extract or recombinant TPX2. Asters formed in a field were counted the error bars represent standard deviations from three independent fields.

TPX2 induces microtubule assembly in Xenopus M-phase extracts

35% ammonium sulphate precipitation contained the highest nucleation activity and were further fractionated by Mono Q and two Mono S columns at different pH. Several proteins correlated with the above peak after these chromatographic steps. Mass spectrometric analysis identified the human homologue of a previously described protein TPX2 (Heidebrecht *et al*., 1997; Wittmann *et al*., 2000) as the most abundant protein in the active fraction (Gruss *et al*., 2001). Addition of 100 nM recombinant TPX2, which is twofold the endogenous concentration (Wittmann *et al*., 2000), was able to restore the aster formation activity of extract depleted by importin α (Figure 14).

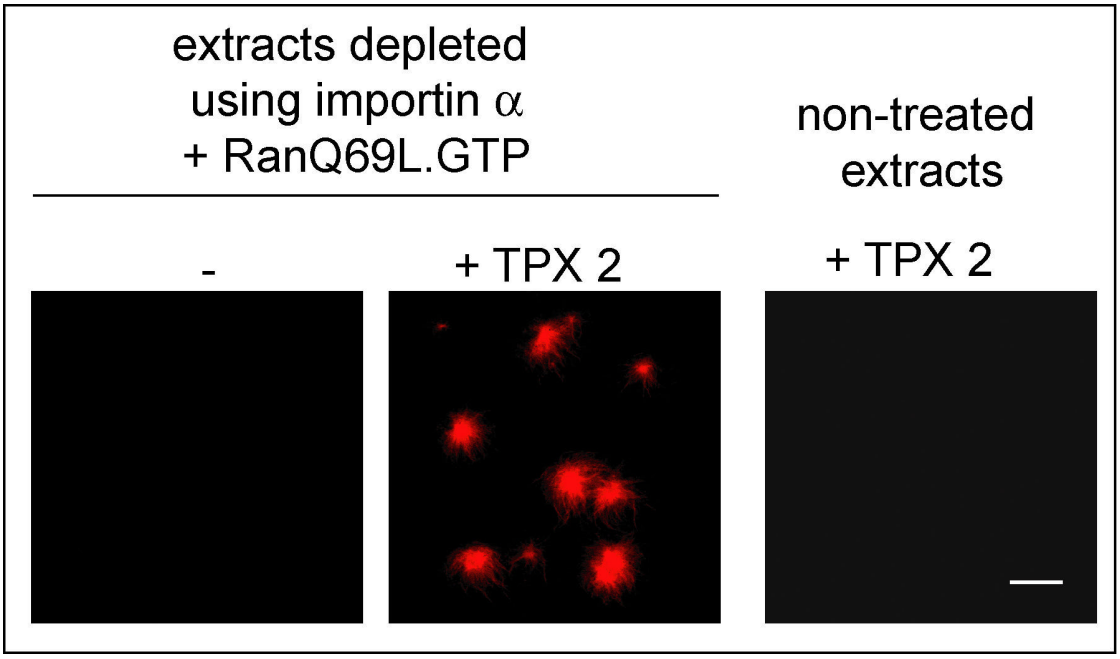

Figure 14. TPX2 restores the activity of extracts depleted of NLS proteins. M phase extracts were depleted using an importin α column in the presence of RanQ69LGTP and microtubule assembly was tested for 20 min without(-) or with(+) 100 nM human TPX2 added. As a control TPX2 was added to wild type extracts (right panel).

These data suggested that in the extract a balance between TPX2 and importin α exists that completely inhibits nucleation. Consequently, excess of TPX2 over importin α should lead to aster formation even in the absence of RanGTP. Indeed addition of 500 nM recombinant TPX2 induced microtubule assembly (Figure 15), this was inhibited by importin α. Hydrolyzing Ran-bound GTP by adding RanGAP and RanBP1 did not stop TPX2 induced microtubule assembly indicating that TPX2 acts downstream of Ran (Figure 15).

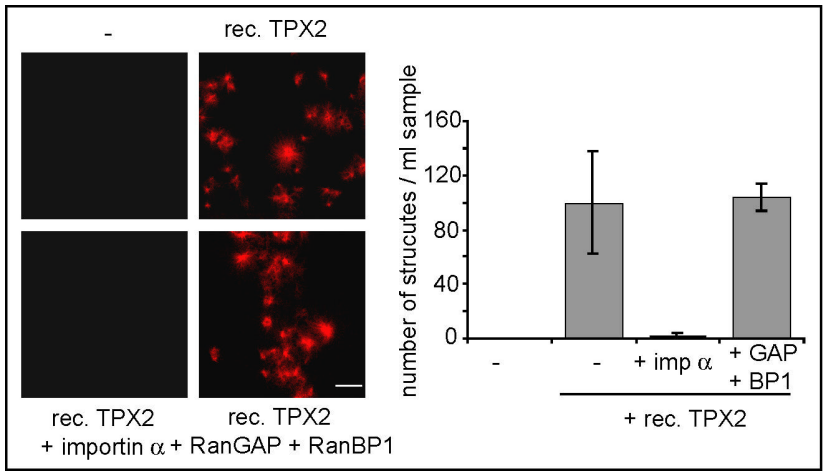

Figure 15. Excess TPX2 is sufficient to assemble microtubules in M-phase extracts. Microtubule assembly was tested in extract supplemented with buffer (-) or 500 nM recombinant TPX2 an 5-fold excess over the endogenous. TPX2 was tested alone or with 30 µM importin α or 5 µM RanGAP and RanBP1. Scale bar is 20 µm.

Our data suggested that TPX2 might indeed be the target of RanGTP in microtubule assembly. To gain further evidence, we tested several predictions of this hypothesis. If TPX2 was the effector of Ran in microtubule nucleation depletion of TPX2 from extract should prevent RanGTP induced microtubule assembly. This was shown to be the case: Extracts depleted of TPX2 were not able to form asters in the presence of RanQ69LGTP (Figure 16). This could be restored by the addition of recombinant TPX2.

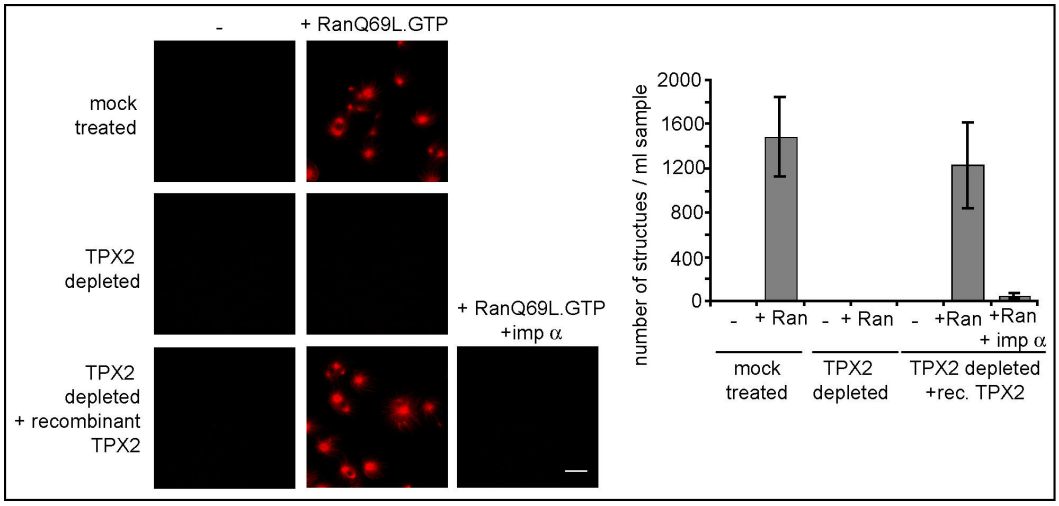

Figure 16. TPX2 is necessary for RanGTP mediated microtubule assembly.

Xenopus M-phase extracts were depleted of TPX2 using affinity-purified antibodies against TPX2 (TPX2 depleted) or rabbit IgG (mock treated), and microtubule assembly tested without (-) or with (+) RanQ69LGTP. To these extracts either buffer (upper panels) or TPX2 (lower panels) was added with or without RanQ69LGTP and or importin α.

TPX2 is required for chromatin induced spindle assembly

It was known that Ran is necessary and sufficient to mediate chromatin induced microtubule assembly (Carazo-Salas *et al*., 1999). Since an excess amount of TPX2 had been shown to be sufficient to assemble microtubules in M-phase extracts (Figure 15) and to be necessary for microtubule assembly by Ran (Figure 16), we were interested whether TPX2 is necessary to mediate this chromatin effect. Extracts were depleted of TPX2 and chromatin beads were added no microtubule assembly around the chromatin beads was observed (Figure 17).

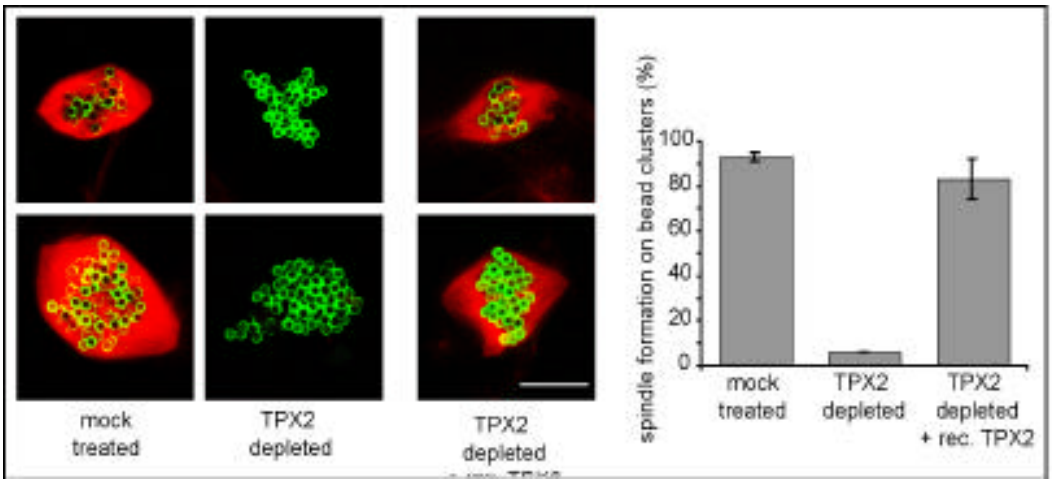

Figure 17. TPX2 is necessary for chromatin mediated microtubule assembly. Chromatin beads were added to extracts depleted of TPX2 or mock depleted with IgG. Either buffer or TPX2 was added and reactions were incubated for 30 min. Percent of bead clusters with a spindle attached to it were counted. Bars represent percent of bead clusters with spindle. Error bars represent standard deviations.

When the TPX2 concentration was restored to endogenous levels by adding recombinant TPX2 chromatin beads were again able to induce microtubule assembly around them (Figure 17). This shows that TPX2 is both necessary for chromatin to assemble microtubule, and, since addition of excess TPX2 alone promoted microtubule assembly in the absence of RanGTP, RCC1 or chromatin (Figure 15) excess TPX2 is also sufficient for microtubule assembly.

While our data identified TPX2 as the downstream target of Ran in microtubule assembly other groups reported NuMA to be a downstream target of Ran (Nachury *et al*., 2001; Wiese *et al*., 2001). The motor protein Eg5 was also shown to increase its plus end movement in the presence of RanGTP (Wilde *et al*., 2001). We wanted to know if those proteins are present at the same levels in extracts passed over an importin α column. We performed western blots on extracts depleted with importin α in the presence of RanGTP and mock treated extracts (Figure 18).

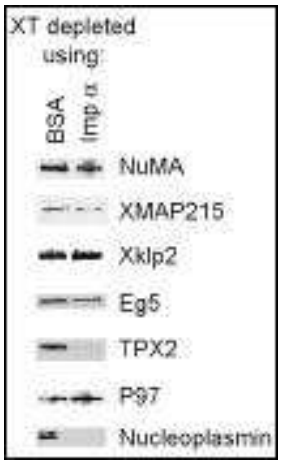

Figure 18. TPX2 is depleted of M-phase extract by immobilized importin α. Extracts were depleted either with protein A-tagged importin α or by BSA as a control. Protein amounts of NuMA, XMAP215, Xklp2, Eg5, TPX2, P97 and nucleoplasmin was compared by Western blot.

The amounts of Xklp2, Eg5, P97 and XMAP215 were not altered by this treatment while TPX2 and nucleoplasmin were depleted by the α column. The level of NuMA was only slightly reduced (Figure 18). This indicates that TPX2 and nucleoplasmin bind tightly to importin α. Other proteins, even though some contain NLS sequences, like NuMA and XMAP215, were only slightly or not reduced by the depletion using immobilized importin α, indicating either that they do not bind as tightly to the import receptor or that they are not in complex with importin α under physiological conditions e.g. as a result of participating in alternative protein complexes. In either case, this suggests that neither NuMA nor Eg5 (Figure 18) are as tightly regulated by Ran and importin α as TPX2 is. Further there was also only one peak of activity, the TPX2 peak, observed in the purification protocol for a microtubule nucleator that responds to importin α regulation in *Xenopus* M-phase extracts, indicating that TPX2 is the strongest nucleator in the HeLa nuclear extracts (Gruss *et al*., 2001). The data however does not rule out that other factors are necessary for microtubule nucleation or that they might also be regulated by Ran.

Analyzing TPX2 induced aster formation

We wanted to know what the physiological role of TPX2 is and in what respect the asters assembled by TPX2 are related to bipolar spindles. When *Xenopus* M-phase extract is provided with sperm nuclei a bipolar spindle forms around the DNA. We wanted to know what the distribution of several spindle associated proteins on TPX2 induced asters is compared to bipolar, sperm-induced, spindles. Asters were assembled in the presence of rhodamine tubulin and stained with antibodies against Eg5, NuMA and γ-tubulin. NuMA and γ-tubulin were detected in the aster centers whereas in bipolar spindles they localize to the spindle poles (Figure 19). Eg5, which localizes along microtubules and to spindle poles in cells (Houliston *et al*., 1994), is present all along the microtubules in TPX2 induced asters

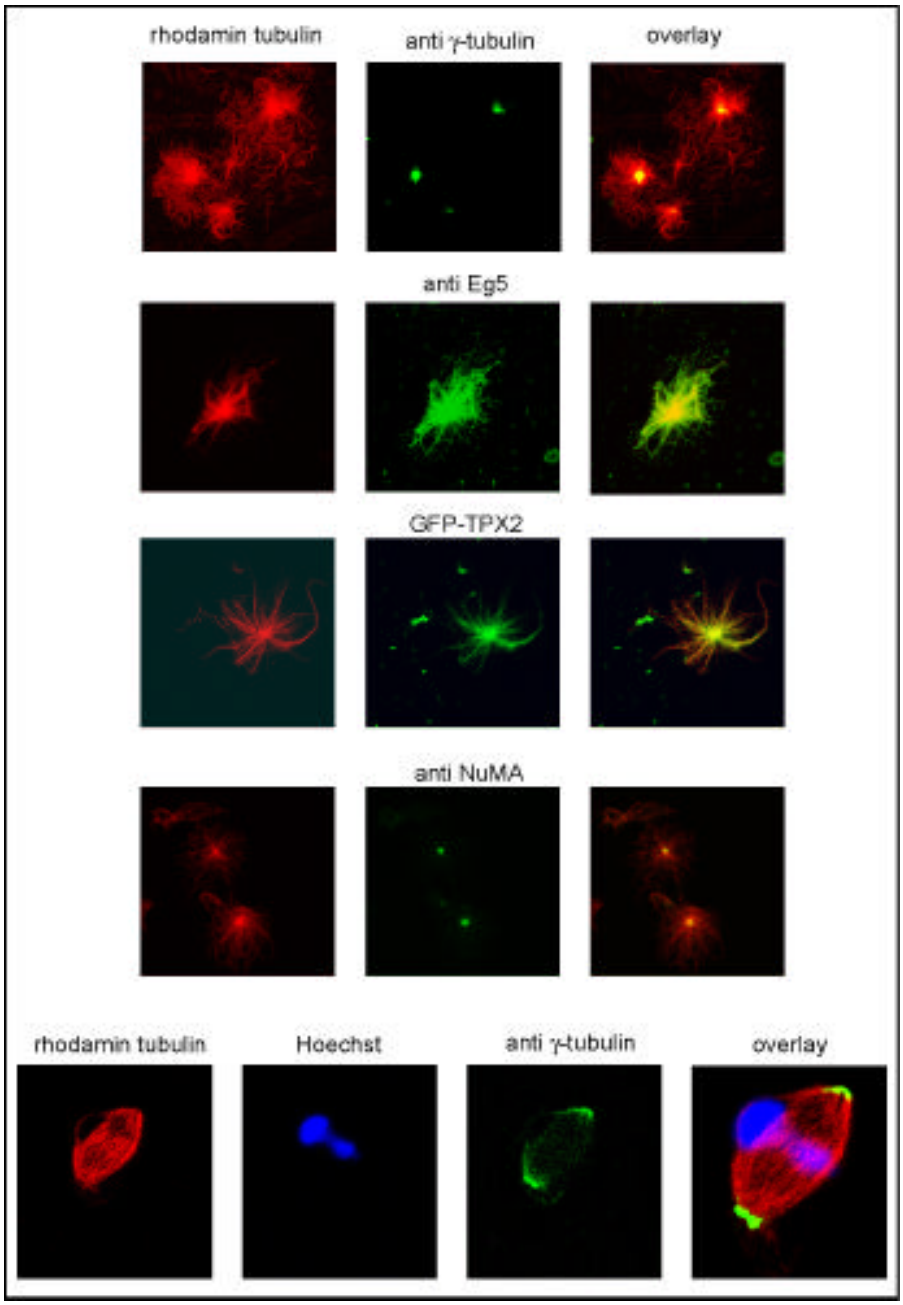

Figure 19. Spindle components localize to TPX2 induced microtubule asters. Microtubule asters were assembled by adding 500 nM TPX2 to egg extracts containing rhodamine-labeled tubulin and samples were incubated for 40 min. Microtubule structures were fixed, spun on cover slips and stained with the antibodies indicated. TPX2 was detected by adding additional 200 nM GFP-TPX2 to the reaction. In the lower

panels spindles were assembled with sperm chromatin in the same way as TPX2 asters. In addition to antibody staining the spindle was stained with the DNA dye Hoechst.

When TPX2 induced asters were either formed in the presence of GFP-TPX2 or stained with anti-TPX2 antibodies TPX2 was detected all along the microtubules (Figure 19). In contrast, although in bipolar spindles TPX2 localizes to the spindle poles in a dynein dependent manner (Wittmann *et al*., 2000). The excess of TPX2 present in these experiments might lead to this difference in localization. Taken together, these results show that the TPX2 asters recruit motors and proteins usually present at spindle poles and centrosomes to the aster centers, suggesting that TPX2-induced asters are organized similarly to the poles of spindles and are thus likely to reflect physiologically relevant processes.

In order to understand which part of TPX2 is necessary to induce microtubule assembly in Xenopus extracts we PCR amplified several fragments of the gene and subcloned them into an expression vector. Proteins were expressed and purified and excess TPX2 fragments were added to Xenopus M-phase extract (Figure 20). The C-terminal fragments of TPX2, TPX2C (240-715) was almost as active in nucleating microtubules as wild type TPX2 while the Δ291(292-715) fragment was even more active than the wild type. A shorter C-terminal fragment Δ434(435-715) was less active in nucleation, an N-terminal fragment TPX2N(1-480) only formed asters at a 10 times higher concentration and a fragment containing the middle part of the TPX2 protein 240-480 was not able to form asters at all. Thus the C-terminal region of TPX2 is sufficient to nucleate microtubules efficiently. The TPX2 N-terminus can however also nucleate microtubule to some extent, indicating a redundancy within the protein.

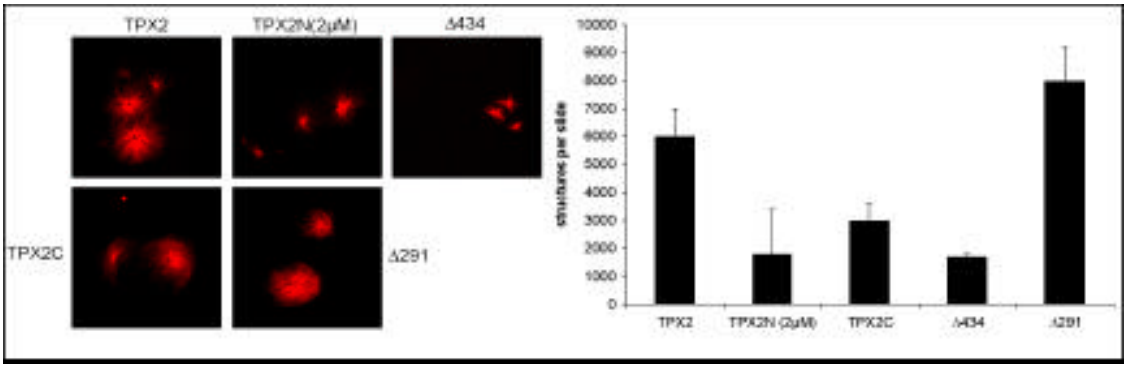

Figure 20. TPX2 fragments induce microtubule assembly in M-phase extracts. TPX2 fragments were PCR amplified , expressed in E. coli, purified and added to M phase extracts at 210 nM (for TPX2N 10 times the amount was used since no structures were observed at 200 nM). The number of structures formed were counted. Error bars represent standard deviations.

In summary the results discussed so far have showed that TPX2 can induce microtubule assembly in *Xenopus* extracts and that this activity is inhibited by importin α. Furthermore, TPX2 acts downstream of Ran and chromatin as the mediator of the "chromatin effect"(Figure 17) and (Gruss *et al*., 2001).

TPX2 binds importin α directly

In order to determine whether binding of importin α to TPX2 is sufficient to regulate TPX2 induced microtubule assembly we characterized the binding of importin α to TPX2 (Figure 21). This would tell us which sequences in TPX2 are necessary for interaction with importin α in M-phase *Xenopus* extracts. Protein A tagged TPX2 was immobilized on IgG sepharose by cross linking and importin α alone, importin β alone or both proteins together were assayed for binding to TPX2 by SDS-PAGE (Figure 21). No binding to a fragemt of Xpo-t, a control protein, or of importin β alone was observed, but strong binding of importin α and β together to TPX2 was observed (Figure 21). Importin α alone also bound to TPX2, but to a lesser extent. From the literature it is known, that the affinity of importin α for at least some NLS cargos is 30 fold higher if it is complexed with

importin β (Harreman *et al*., 2002). This effect probably explains the better binding of α/β to TPX2 compared to α alone. Interestingly, faster running importin α bands are enriched in the lane where importin α is assayed for binding to TPX2 alone (Figure 21). These bands represent N-terminal degradation products of importin α, which lack the IBB domain and bind better to TPX2 without importin β. The IBB domain binds to importin β but also auto-inhibits NLS binding to α unless β is bound (Harreman *et al*., 2002). The truncated importin α does not have this auto-inhibition domain and therefore can bind NLS cargo more efficiently than the full-length protein in the absence of importin β.

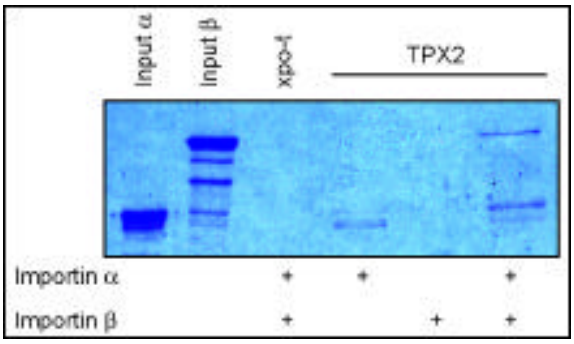

Figure 21. TPX2 binds to importin β through importin α. TPX2, or an Xpo-t fragment as a control, was immobilized on IgG-Sepharose and importin α or importin β alone or both proteins together(indicated by +) were tested for binding. Shown is a Coomassie-stained SDS-PAGE gel of column bound fractions.

TPX2 has one critical binding site for importin α

To further characterize the importin α-TPX2 interaction we wanted to identify the binding site for importin α in TPX2. The computer program NUCDISC can predict classical NLS mono and bipartite nuclear localization sequences based on an algorithm which compares short peptide stretches with known NLS motifs. 7 putative monopartite NLS, which we considered possible interaction sites for importin α, were predicted in TPX2 (Figure 22).

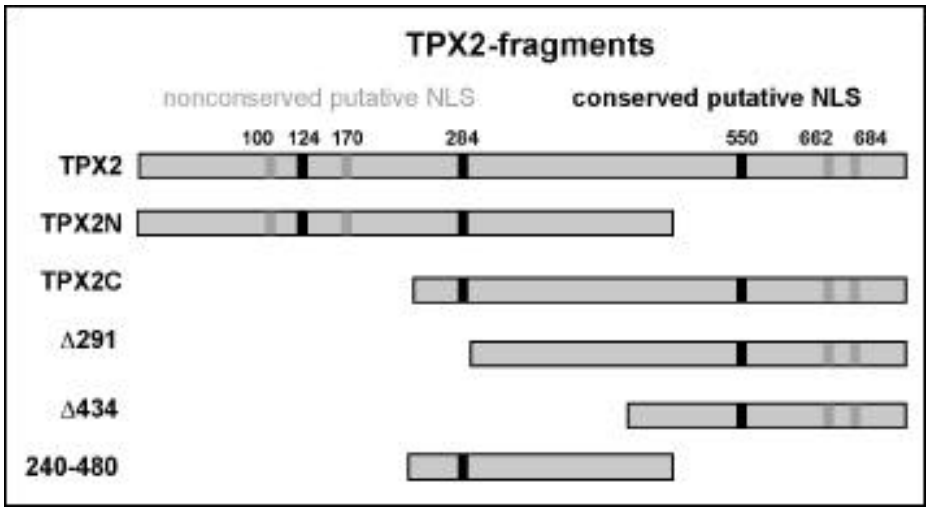

Figure 22. TPX2 contains three putative NLS. The computer program NUCDISC (Nakai and Horton, 1999) was used to identify predicted Nuclear Localisation Signals (NLSs) in the *Xenopus* TPX2 cDNA. Conserved putative NLSs are shown as black boxes, non-conserved as light grey boxes. The panel shows different fragments of the *Xenopus* TPX2 cDNA which were expressed in *E. coli*. Numbers represent amino acids positions in the full-length protein.

Three of these seven sites were conserved between *Xenopus*, mouse, chicken and man. To test whether the conserved predicted NLSs were indeed importin α binding sites fragments of TPX2 were PCR amplified and subcloned into an expression vector introducing a protein A tag. The TPX2 fragments were expressed, purified and immobilized on an IgG column and importin α was assayed for binding to these columns (Figure 23). Binding of importin α was observed to both a C-terminal fragment (aa 240-715) and an N-terminal fragment (aa 1-480) a control protein, a fragment of Xpo-t, did not show any binding. A C-terminal fragment which was slightly shorter (Δ291, aa 292-715) than TPX2C as well as the Δ434 (aa 435-715) did not bind importin α anymore (Figure 23) indicating that amino acids 280-291 are important for α binding.

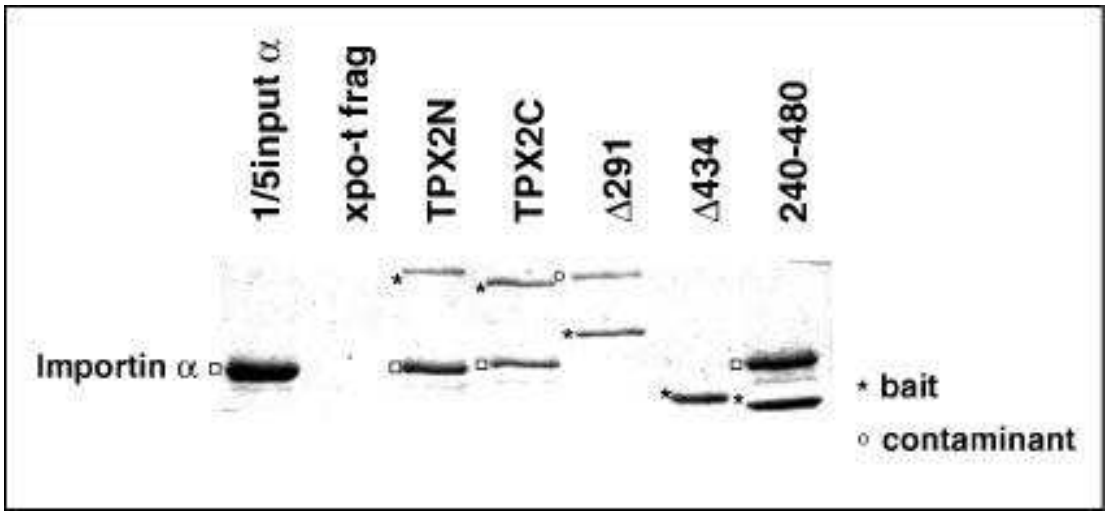

Figure 23. A central region in TPX2 is essential for binding to importin α. TPX2 derivatives were immobilized on IgG-Sepharose and importin α binding was tested. Shown is a Coomassie-stained SDS-PAGE gel of column-bound fractions which had been eluted with 2 M $MgCl_2$. The bait proteins are marked with an asterisk, bound importin α as an open square, the Δ291 lane contains a contaminant marked with an open circle. Note that due to its tight binding to IgG Sepharose the Xpo-t fragment is not eluted with 2 M $MgCl_2$, although similar amounts of all bait proteins had been coupled to IgG Sepharose as seen after elution with SDS and Coomassie staining (data not shown).

In order to further define the importin α binding site in TPX2 point mutations centered at the putative NLS sites at amino acids 124, 284 and 550 were introduced by mutagenic PCR and basic amino acids were changed into alanines both in the context of the full length protein and in the context of the TPX2C fragment (aa 240-715) (Figures 24 and 25). Mutation at position 550 (TPXC550) did not affect importin α binding to the C-terminus of TPX2 (Figure 24) whereas mutation at residue 284 (TPXC284) disrupted importin α binding (Figure 24). In the context of full length TPX2, mutation of two basic residues (aa 284, 285) to alanines was sufficient to prevent importin α binding to TPX2 (Figure 25), indicating that the region encompassing these two amino acids is critical for the

interaction, while mutation at position 124 did not change the binding properties of TPX2.

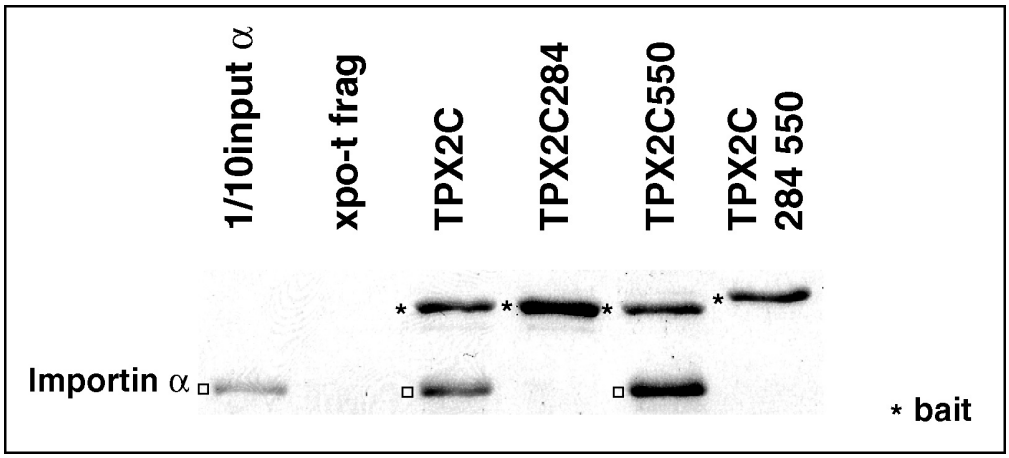

Figure 24. One site in the C-terminus of TPX2 is critical for binding to importin α. Point mutants of the C-terminal fragment of TPX2 were tested for importin α binding. TPX2 fragments are immobilized on a column and importin α was assayed for binding by SDS-PAGE.

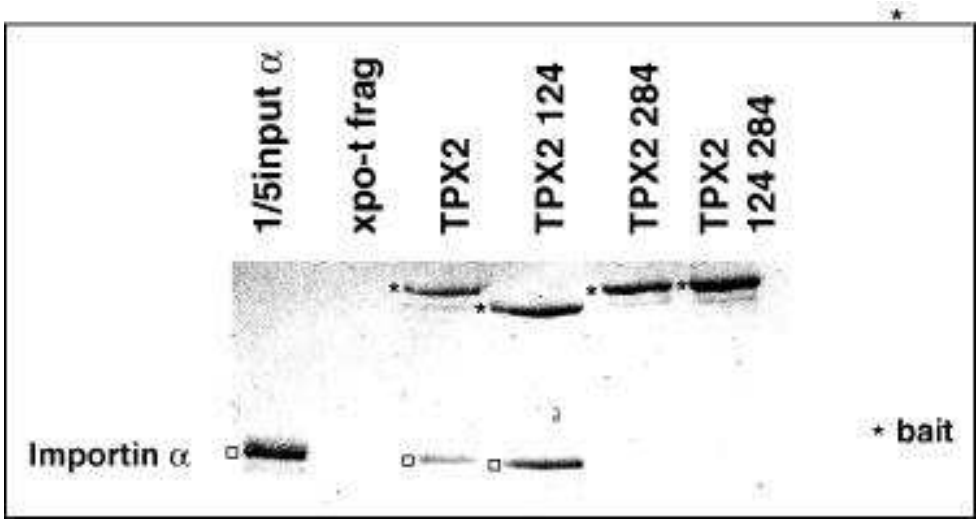

Figure 25. A point mutation centred at aa 284 in TPX2 is critical for binding to importin α. Point mutants of the full-length TPX2 protein were tested for importin α binding. TPX2 was immobilized on a column and importin α was assayed for binding by SDS-PAGE.

TPX2 function in microtubule assembly is directly regulated by importin α.

In order to test whether importin α binding regulates TPX2 directly, the TPX2 mutants were tested for their ability to nucleate microtubules in egg extracts. All tested mutants induced aster formation (Figure 26). Both the wild type TPX2 protein as well as the 124 mutant protein were inhibited by the addition of excess importin α (Figure 26 A). TPX2 variants mutated at position 284, which did not bind to importin α in the pull down experiment (Figure 25), were, however, able to induce aster formation even in the presence of excess exogenous importin α (Figure 26 A). This indicated that the sequence around position 284 is both essential for the binding of importin α and for the inhibitory interaction of TPX2 with importin α.

We than wanted to know whether the importin α interaction is sufficient to regulate TPX2. Endogenous TPX2 protein was immunodepleted from *Xenopus* M-phase extract and then reconstituted with either wild-type TPX2 or the TPX2

284 mutant (Figure 26 B). In a wild type egg extract the endogenous importin α should be sufficient to inhibit the endogenous TPX2 and no microtubule asters should be formed in the absence of RanGTP. Indeed when 20 nM wild type TPX2 protein was added back to the immunodepleted extract no microtubule assembly was induced (Figure 26 B). In contrast, 20 nM of the 284 mutant variant of TPX2 that is unable to bind importin α efficiently induced aster formation (Figure 26 B). Furthermore, the presence of the non-hydrolysing RanQ69L mutant in its GTP-bound form (RanQ69LGTP) enabled wild-type TPX2 to nucleate aster formation efficiently but did not increase the number of asters nucleated by the mutant TPX2 (Figure 26 B). This indicated that the wild-type protein was active only once released from importin α by RanGTP but that the TPX2 284 mutant was constitutively active in microtubule assembly. Thus, TPX2 has one critical importin α binding site whose mutation renders it able to constitutively induce microtubule assembly in egg extract and prevents its regulation by RanGTP.

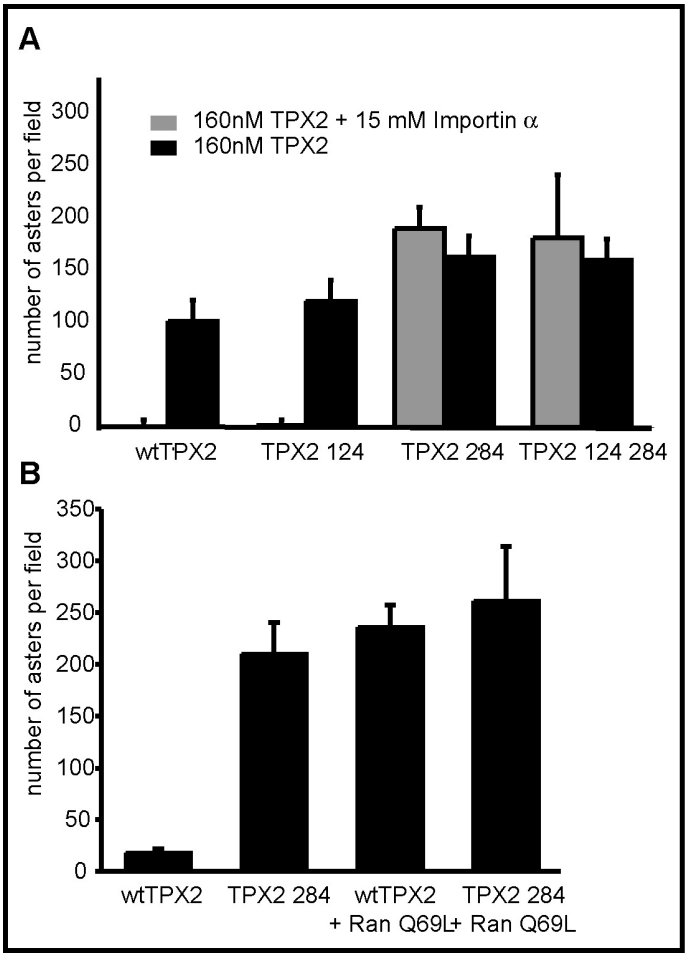

Figure 26. TPX2 function in microtubule assembly is directly regulated by importin α.

(A) TPX2 mutants were tested for their ability to nucleate microtubules on addition to *Xenopus* M-phase extract to a concentration of 160 nM in the presence of rhodamine-labeled tubulin. Results were quantified by counting structures from three fixed and squashed samples (Sawin and Mitchison, 1991). Error bars represent standard deviations. All tested mutants were able to induce assembly of aster-like structures (black histograms). Addition of importin α (light grey histograms) inhibited assembly of microtubules induced by either the wild-type TPX2 (wt) protein or the 124 mutant protein, but not by the 284 mutant protein or the double mutant TPX2 124 284.

(B) *Xenopus* M-phase extract was depleted of endogenous TPX2 protein and either wild-type TPX2 protein or TPX2 284 was added in recombinant form to a concentration of 20

nM. The wild-type TPX2 did not induce microtubule assembly. TPX2 284, on the other hand, was able to form asters at the same concentration. A GTP hydrolysis-deficient mutant form of Ran (Q69L) in its GTP-bound form enabled wild-type TPX2 to nucleate a similar number of asters but did not increase the number of asters nucleated by the mutant TPX2 (TPX2 284).

TPX2 is a microtubule nucleator *in vitro*

Since TPX2 induces microtubule assembly in Xenopus M phase extracts we whished to determine whether it has a direct effect on *de novo* microtubule formation. To test the possibility of TPX2 being a microtubule nucleator it was added to different concentrations of purified porcine tubulin in buffer (Figure 27). The mixture was incubated at 37 °C for 12 min and then fixed. In these assays, the human TPX2 protein was used as it is easier to produce in soluble recombinant form. 800 nM TPX2 were able to induce small aster like structures when incubated with 5 µM tubulin (Figure 27). When higher amounts of tubulin (20 µM) were used in the experiment organized and bundled microtubule structures were efficiently induced (Figure 27). When buffer instead of TPX2 was added to the reaction very few microtubules assembled spontaneously at this lower tubulin concentration. This indicates a specific effect of TPX2 on microtubule assembly and organisation (Figure 27).

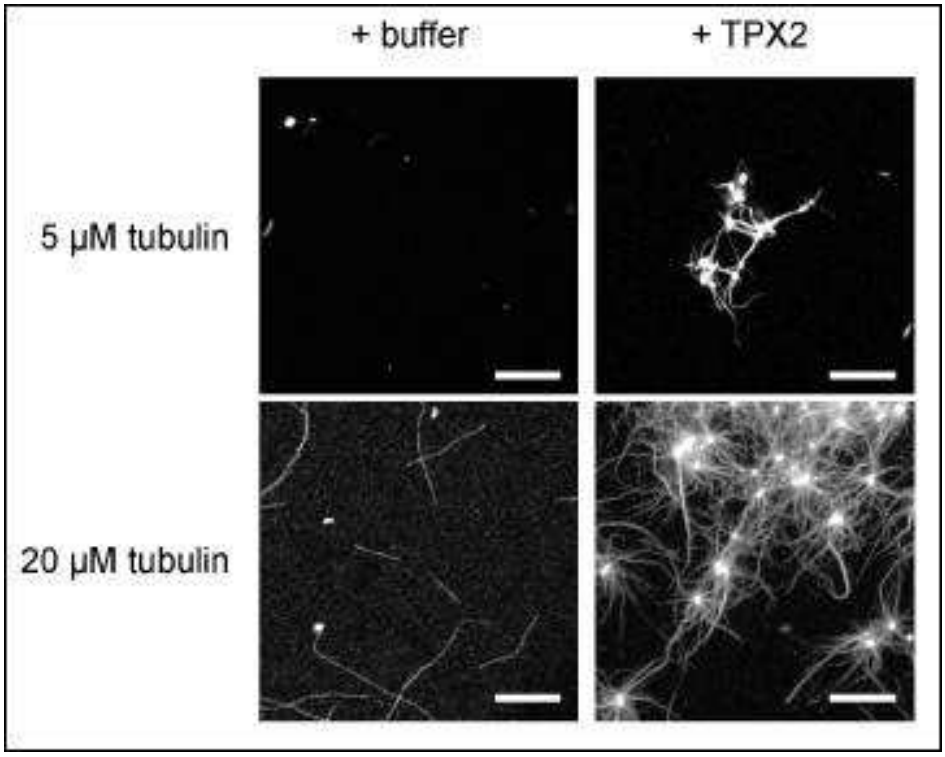

Figure 27. *In vitro* TPX2-induced microtubule nucleation.

Addition of TPX2 to different concentrations of purified porcine tubulin (5 µM, upper panels, 20 µM, lower panels) induced the assembly of aster-like structures containing bundled microtubules (right panels), unlike tubulin alone (left panels). (B) Bar: 10 µm.

TPX2 induces aster seed formation through microtubule nucleation and bundling

We were curious how the TPX2 induced structures look in detail and where on these asters the TPX2 protein was localized. In order to get high resolution images of the astral microtubules we used cryo-electron microscopy. Microtubule structures were induced in the same way as described for the light microscopy above (Figure 28). Two structural features were observed. The first were amorphous aggregates of varying size, which only formed in the presence of both TPX2 and tubulin (data not shown). Microtubules emanated randomly in all directions from these aggregates (Figure 28, arrows indicate aggregates in D

while smaller aggregates are seen in A, B). Many structures contained an array of colinear microtubules, which overlapped and bent at the region corresponding to the aster centre (Figure 28 A-C). To visualise TPX2 in these structures, we used a protein A tagged version of human TPX2 (hTPX2), which could be visualised by 5 nm colloidal gold particles coated with antibody. Gold labelling was seen both on the aggregates and along the microtubules growing outwards from these aggregates (Figure 28D). No preferential gold labelling could be detected at the ends of microtubules. Note that we are not able to distinguish between the microtubule plus and minus end in this experiment. In *Xenopus* extracts TPX2 was observed both bound along microtubules and on spindle poles (Wittmann *et al*., 2000). Immuno-gold labelling of TPX2 on microtubule structures induced by TPX2 in vitro confirm the localization along microtubules. We do not see preferential binding to the aster poles indicating that other proteins from the extract, in particular dynein, are essential to accumulate TPX2 on spindle poles (Wittmann *et al*., 2000).

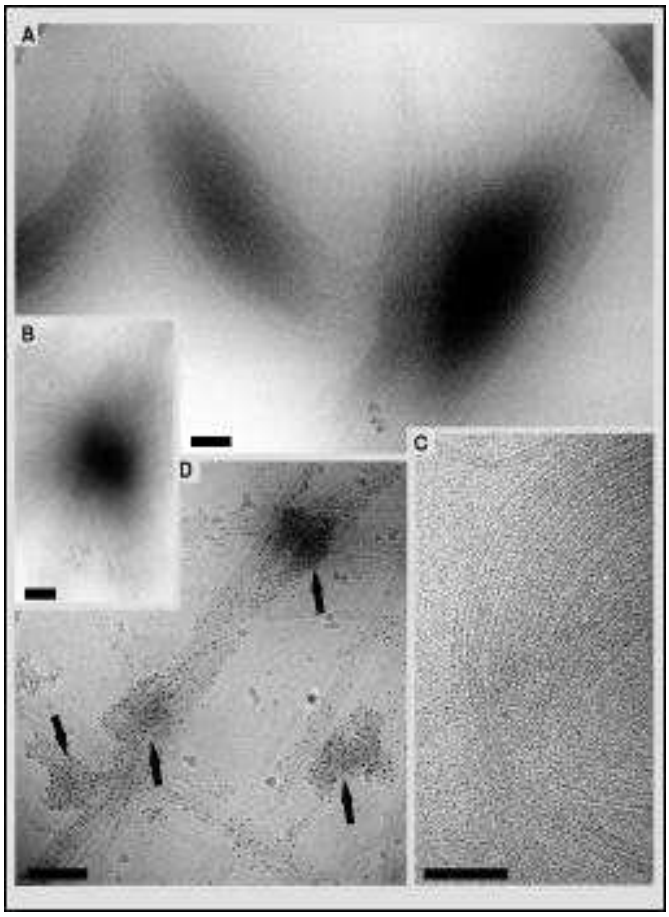

Figure 28. Visualisation of TPX2-mediated microtubule assemblies by cryo-electron microscopy. (A-C) Recombinant zz-tagged TPX2 (0.8 µM) was incubated for 10 minutes at 37 °C with 5 µM purified tubulin in BRB80. Reactions were directly spotted on copper grids, washed, shock-frozen and structures were visualized as described (Dubochet *et al.*, 1985).
(D) Reactions were performed in the presence of 5 nm-gold-labelled anti-rabbit IgG to visualise zz-tagged TPX2. Bar: 200 nm.

Differential regulation of the nucleation and bundling activities of TPX2 by importin α

In *Xenopus* egg extract TPX2 function in microtubule assembly is regulated by importin α. To investigate whether TPX2 is also regulated by importin α in a

minimal system consisting only of recombinant TPX2, importin α/β and tubulin either wild-type importin α or the "ED" mutant form of importin α, which was described above, were added to the assembly reaction together with importin β (Figure 29). TPX2, if added alone, induced the formation of aggregates from which microtubules emanated (Figure 29). On the other hand only the aggregates were observed when TPX2 was added to tubulin in the presence of importin α and β. This inhibition was specific since addition of the same concentration of the ED mutant with importin β had little effect on TPX2 microtubule nucleation (Figure 29). A mutant form of hTPX2, in which the equivalent NLS sequence to that in *Xenopus* TPX2 284 was mutated, hTPX2 315, was not able to bind importin α when tested in a pull down assay (data not shown), but the protein was as active as the wild-type in inducing microtubules. Addition of importin α had little effect on hTPX2 315 ability to assemble microtubules, again indicating that the inhibition by importin α is specific. (Figure 29). Thus, importin α and β regulate the ability of TPX2 to induce microtubule assembly in the purified system as they do in the complete egg extract. Importin α alone also inhibited TPX2-induced microtubule assembly, but less efficiently than together with importin β, as expected from the pull down experiments (Figure 29).

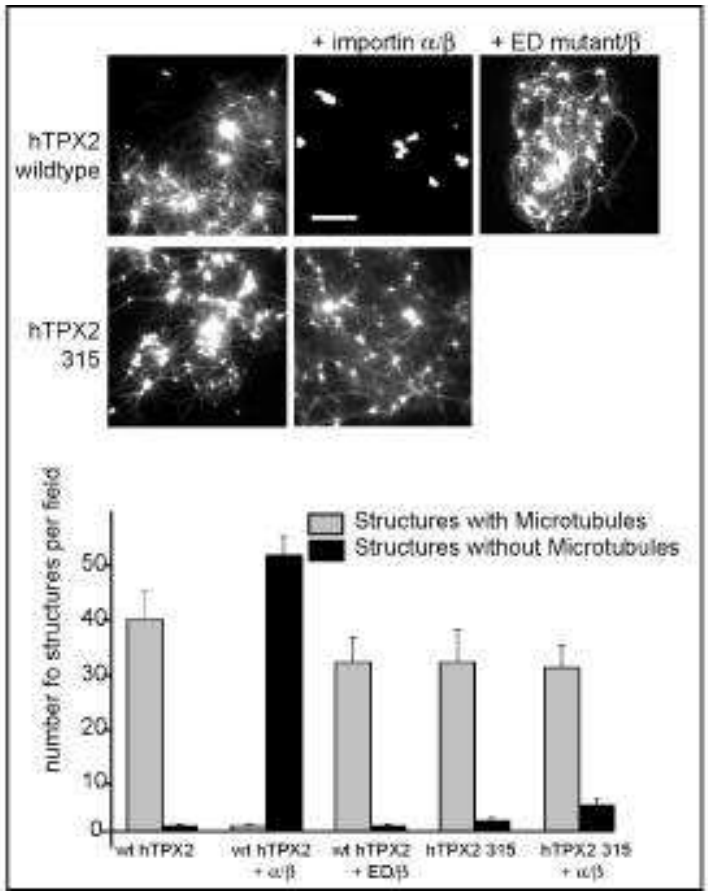

Figure 29. TPX2 is regulated by importin α in the purified reaction

(A) wt-hTPX2 (upper panels) induced both tubulin/TPX2 aggregates and outgrowing microtubules. Addition of importin α and β (upper middle panel) but not of the ED mutant protein and importin β (upper right panel) inhibited microtubule outgrowth, but aggregates were still observed. A mutant form of hTPX2 lacking the importin α binding site (TPX2 315, lower panels) induced microtubule asters (lower left panel), but its activity was not affected by importin α and β (lower right panel). Bar: 10 µm. (B) Aggregates with microtubules attached (light grey histograms) and aggregates with no microtubules attached (black histograms) were counted in at least 10 fields. Error bars represent standard errors.

One possibility by which importin α could inhibit microtubule nucleation by TPX2 is through sterically hindering TPX2 binding to tubulin. To test this, hTPX2 or hTPX2 315 were incubated with taxol-polymerised microtubules in the presence or absence of importin α and β (Figure 30). The microtubules were then spun

through a sucrose cushion and, after separation of the pelleted material by SDS-PAGE, Western blot was used to detect the bound TPX2 (Figure 30). The same amount of TPX2 was seen to co-pellet with microtubules in the presence or absence of the importins (Figure 30, lanes 2 and 3). Thus, although the ability of TPX2 to nucleate microtubules is abolished by importin α, the binding of TPX2 to pre-polymerized microtubules is not prevented.

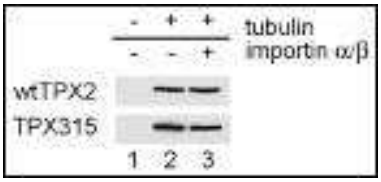

Figure 30. TPX2 binds to microtubules independent of importin α.

Wild type hTPX2 or mutant hTPX2 (hTPX2 315) was incubated with or without taxol polymerized microtubules in the presence or absence of importin α and β as indicated, samples were pelleted and TPX2 detected in pellet fractions by SDS-PAGE and Western blotting.

Several MAPS have the ability to bundle microtubules (Andersen and Karsenti, 1997b). The electron microscopy of TPX2-induced microtubule asters suggested that TPX2 could also bundle microtubules. We wished to test whether TPX2 can induced bundling and whether that would also be regulated by importin α/β. Microtubules were assembled in the presence of taxol and then diluted in taxol-containing buffer and cooled to avoid further microtubule polymerisation (Figure 31) Under the conditions of this experiment, single microtubules are not observed. Addition of TPX2 caused the pre-polymerised microtubules to form bundles (Figure 31). This bundling activity was unaffected by the addition of importin α and β (Figure 31) even when a large excess over TPX2 was added. This suggests that TPX2 ability to bind microtubules and to bundle them is not affected by importin α/β.

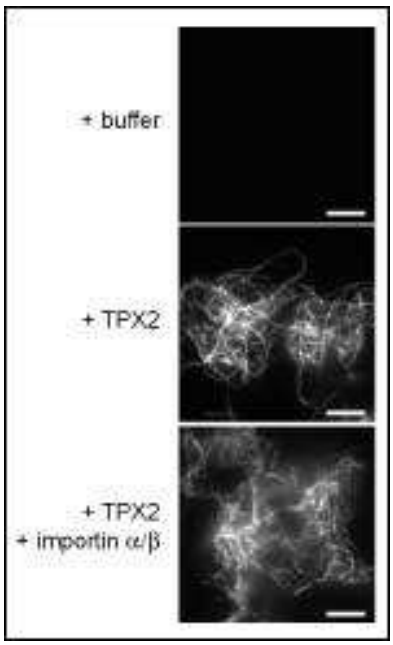

Figure 31. TPX2 bundles microtubules independent of importin α. Microtubules were polymerized from a solution of 40 µM tubulin in the presence of taxol and diluted 1:40. Either buffer alone (top panel), 0.2 µM TPX2 (middle panel), or TPX2 and both 5 µM importin α and importin β (lower panel) were added. Bar: 10 µm. Note that the conditions of the microscopy were such that individual microtubules were not visible.

Ran induced spindle organization is a two step mechanism

It has been reported previously that Ran not only promotes aster assembly in *Xenopus laevis* M-phase extracts but also organizes microtubules into spindle like structures (Carazo-Salas *et al*., 1999; Wilde *et al*., 2001). The Ran-induced structures are oriented towards each other and show two or more poles. We wanted to know whether TPX2 is part of the pathway leading to spindle-like structures by Ran. Alternatively, other factors might be involved. These factors might be regulated by importin α, like TPX2, or linked to the Ran system in a different way. In order to do so we took advantage of the ΔNLSTPX2 protein. In M-phase *Xenopus* extracts TPX2 alone forms asters, addition of RanGTP leads

to organized spindle-like structures. When instead of wild type TPX2 protein the ΔNLS mutant TPX2 is used, asters are formed even in the presence of exogenous importin α (Figure 34). In the presence of exogenous importin α, addition of RanGTP did not lead to spindle assembly (Figure 34). This indicates that spindle formation induced by Ran is a two step process. The first step is aster formation, performed by TPX2 and regulated by Ran and inhibited by importin α. The second step is organizing these asters into spindle-like structures, also regulated by Ran and importin α, but not triggered by TPX2 (Figure 35). The ability to dissect Ran-induced spindle formation into two steps should allow to screen for factors promoting the organising step. An activity which organizes asters into spindle like structures has been predicted by computer simulations to require both plus and minus end directed motors (Nedelec *et al*., 2003). One of the factors known to be necessary for organisation is the motor protein Eg5, which cross links anti parallel microtubules (Gaglio *et al*., 1996). Further work will hopefully identify the proteins involved in the process.

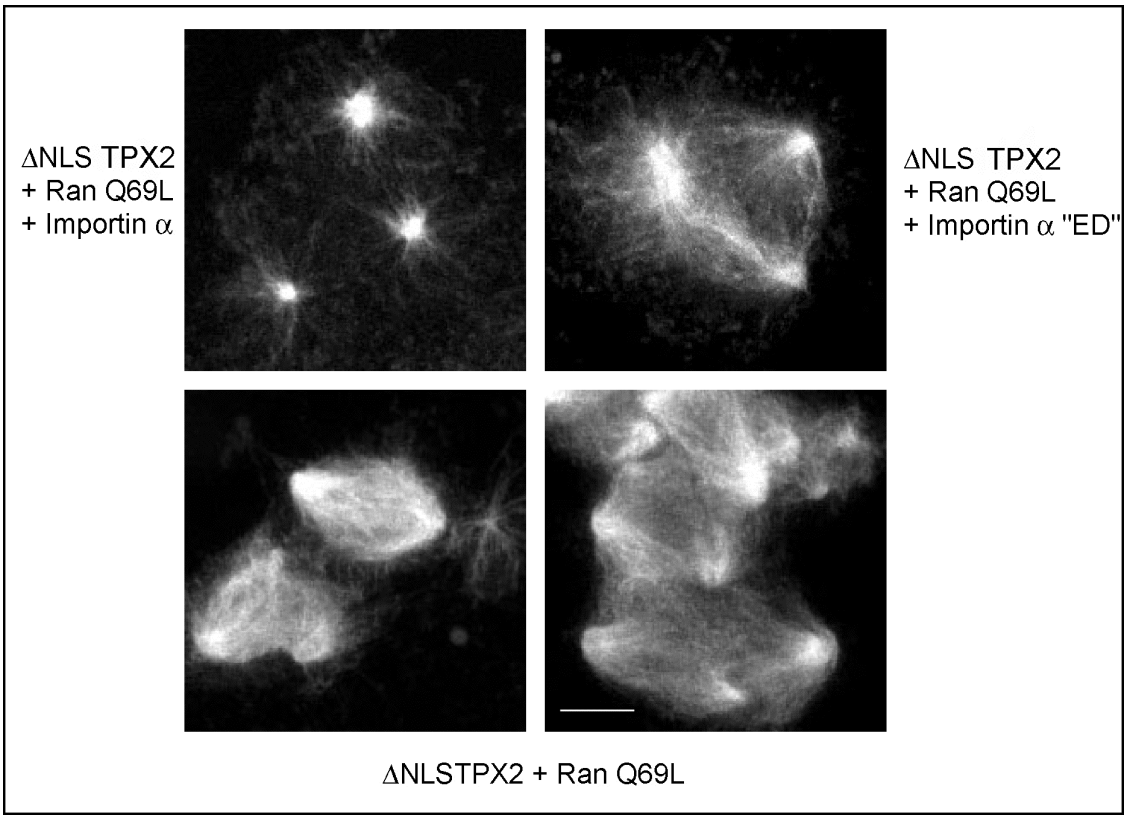

Figure 34. Importin α acts to inhibit spindle organization independent of TPX2.

Microtubule assembly was tested in M phase arrested *Xenopus* egg extracts in the presence of rhodamine-labeled tubulin for 30 min after incubation with RanQ69LGTP, ΔNLSTPX2 and either buffer, importin α or importin α "ED" mutant as indicated. Scale bar 5 µm

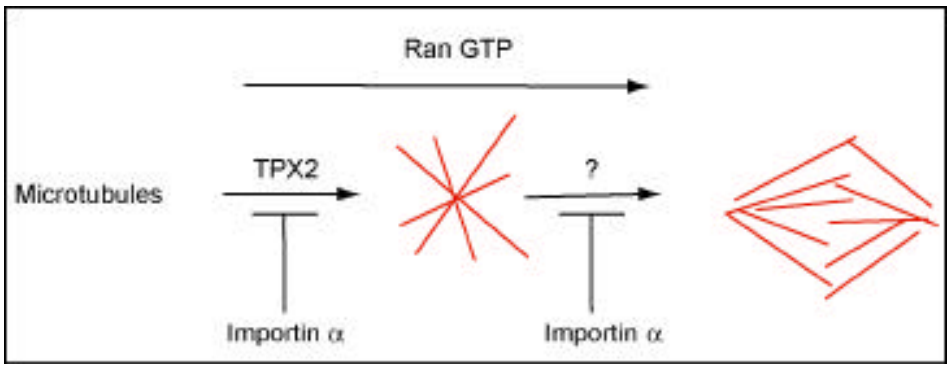

Figure 35. Model for Ran induced organization of spindle-like structures

RanGTP induces spindle-like structures in *Xenopus* M phase extracts in a two step process. The first step is promoted by TPX2 and leads to aster assembly, the second step is dependent on an unknown activity and leads to pole formation. Both steps can be inhibited by importin α.

TPX2 is necessary for Ran induced centrosome activation

Sperm centrioles do not have pericentriolar material, which is necessary for their ability to nucleate microtubules, they recruit it upon entry into the egg. Similarly to what happens after fertilization, when sperm nuclei are added to egg extract sperm centrioles recruit pericentriolar material such as γ-tubulin from the extract and only then are able to nucleate microtubules (Stearns and Kirschner, 1994). During mitosis centrosomes nucleate at least five times more microtubules than do interphase centrosomes (Paoletti and Bornens, 1997). The change in nucleation capacity that accompanies the G2/M transition has been termed centrosome maturation. On the other hand it has been previously shown that the amount of tubulin nucleated by sperm centrosomes is increased in the presence of RanGTP (Carazo-Salas *et al*., 2001) and it was suggested that activation of centrosomes by RanGTP resembles centrosome maturation (Carazo-Salas *et al*., 2001). We wanted to confirm the published effect of Ran on nucleation by

centrosomes and wanted to find out if importin α or TPX2 also play a role in this process. De-membranated sperm were incubated in an extract supplemented with either buffer as a control, RanBP1 and RanGAP to hydrolyse all endogenous Ran bound GTP, or RanQ69LGTP. The extracts contained nocodazole, a drug which depolymerizes microtubules and prevents microtubule nucleation in the extract but should allow recruitment of proteins from the extract to the sperm centrioles. We then re-isolated the sperm heads (Felix *et al*., 1994) and incubated them in a solution of pure tubulin (Buendia *et al*., 1992; Carazo-Salas *et al*., 2001). Images of asters were taken on a wide field microscope and the total fluorescence was measured by a macro written for the NIH Image software (Figure 36). The total fluorescence directly represents the microtubule mass in this experiment. Since microtubule nucleation was performed in a solution of pure tubulin without MAPs and for the same time the microtubule mass is a measurement of the nucleation capacity of the centrosomes. Images of asters are shown in the upper part of Figure 36, lower panels show the number of asters with a certain total fluorescence. The nucleating capacity of centrosomes incubated in the presence of RanQ69LGTP is three times higher compared to those incubated in the presence of buffer alone (mean fluorescence of 3842 compared to 1247 Figure 36). When the endogenous RanGTP is hydrolysed, the nucleating capacity decreases even further (mean fluorescence of 733 Figure 36) indicating that endogenous RanGTP increases the nucleation capacity of centrosomes.

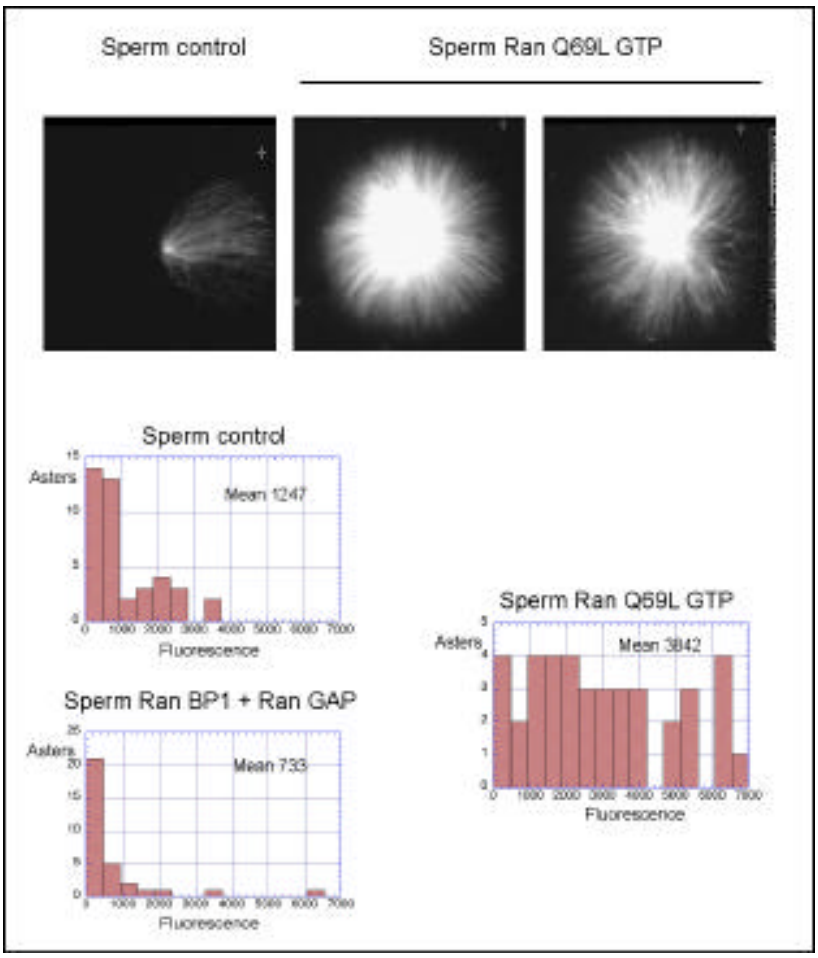

Figure 36. Ran increases microtubule nucleation by sperm centrosomes.

Sperm centrosomes were incubated in *Xenopus* M phase extract in the presence of nocodazole, reisolated and tested for their ability to nucleate microtubules in a solution of pure tubulin. The experiment is performed in the presence of 30 µM RanQ69LGTP, buffer alone, or 10 µM RanBP1 and RanGAP. Pictures are taken on a wide field microscope. Quantification is based on total fluorescence as an indicator for microtubule mass.

Since RanGTP activates centrosomes we wanted to test whether Ran acts as it does during nucleocytoplasmic transport and whether importin α acts as an inhibitor in the process. Sperm heads were incubated in M phase egg extracts with buffer or RanQ69LGTP either alone or after addition of 30 µM importin α was added. Again the mean fluorescence increased in the presence of RanQ69LGTP compared to control but was significantly reduced upon addition of importin α (mean fluorescence of 2810 compared to 1934 and 1855 Figure 37). Also in the control experiment with buffer the centrosome activity was further reduced by the addition of importin α (mean fluorescence of 1440 Figure 37). This indicates that importin α serves as an inhibitor of a factor necessary for centrosome activation and this factor is released from importin α by RanGTP.

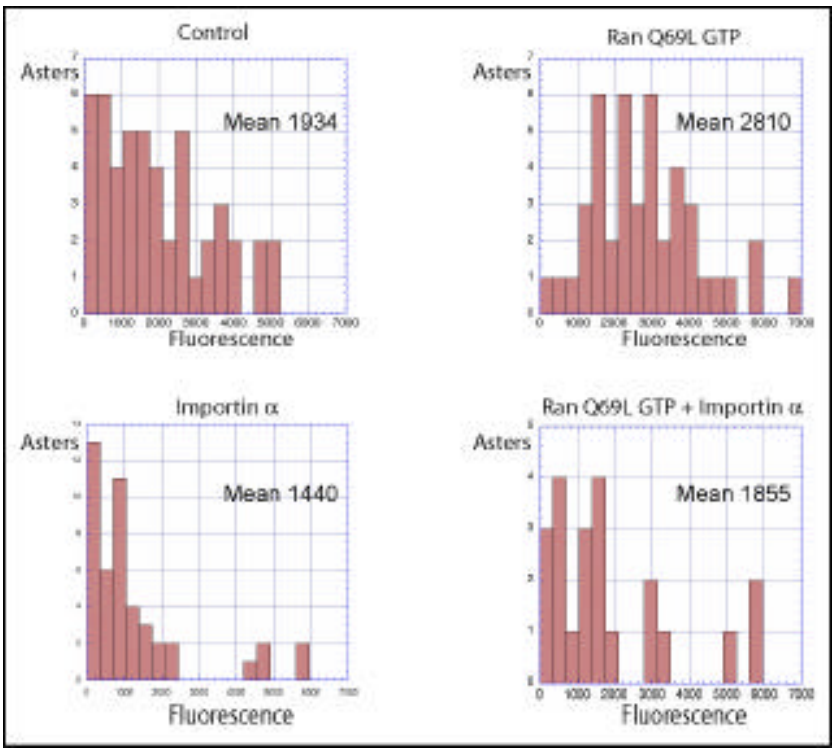

Figure 37. Importin α inhibits Ran stimulation of microtubule nucleation by sperm centrosomes.

Sperm centrosomes were incubated in *Xenopus* M phase extract in the presence of nocodazole, reisolated and tested for their ability to nucleate microtubules in a solution of pure tubulin. The experiment is performed in the presence of 30 µM RanQ69LGTP, or buffer. In the lower panels 30 µM importin α is added to the reactions. Quantification is based on total fluorescence as an indicator for microtubule mass

One protein shown to be regulated by Ran in this way is TPX2. We therefore wanted to test whether TPX2 is necessary for Ran mediated centrosome activation. We depleted TPX2 from *Xenopus* extract and then added sperm centrosomes in the presence or absence of RanGTP, repurified them, and assayed their ability to nucleate microtubule in buffer with pure tubulin (Figure 38). Centrosomes incubated in mock treated extracts gained roughly two times

more nucleating capacity in the presence of RanGTP compared to the control with RanBP1 and RanGAP (mean fluorescence of 5548 compared to 3217 Figure 38). When centrosomes were incubated in TPX2-depleted extracts the asters were three times smaller (mean fluorescence of 1129 compared to 3217 Figure 38). Even in the presence of RanQ69LGTP asters repurified from TPX2 depleted extracts were two times smaller than asters from Mock treated extracts in the presence of RanBP1 (mean fluorescence 2372 compared to 5548 Figure 38). This indicates that TPX2 is necessary for Ran mediated activation of centrosomes. It might be that high amounts of RanGTP in the extract release TPX2 from importin α, which then binds to centrosomes, leading to an increased nucleating capacity in pure tubulin. However, it is not clear whether this happens in living cells since no major defects in nucleation by centrosomes were observed in HeLa cells depleted of TPX2 by RNAi, although fragmentation of centrosomes is sometimes observed (Garrett *et al*., 2002 and Thomas Kufer personal communication; Gruss *et al*., 2002). The increase between RanBP1 treated and RanQ69L treated TPX2 depleted extracts (Figure 38) could be explained by other Ran activated factors involved but might also be is due to an incomplete depletion of TPX2.

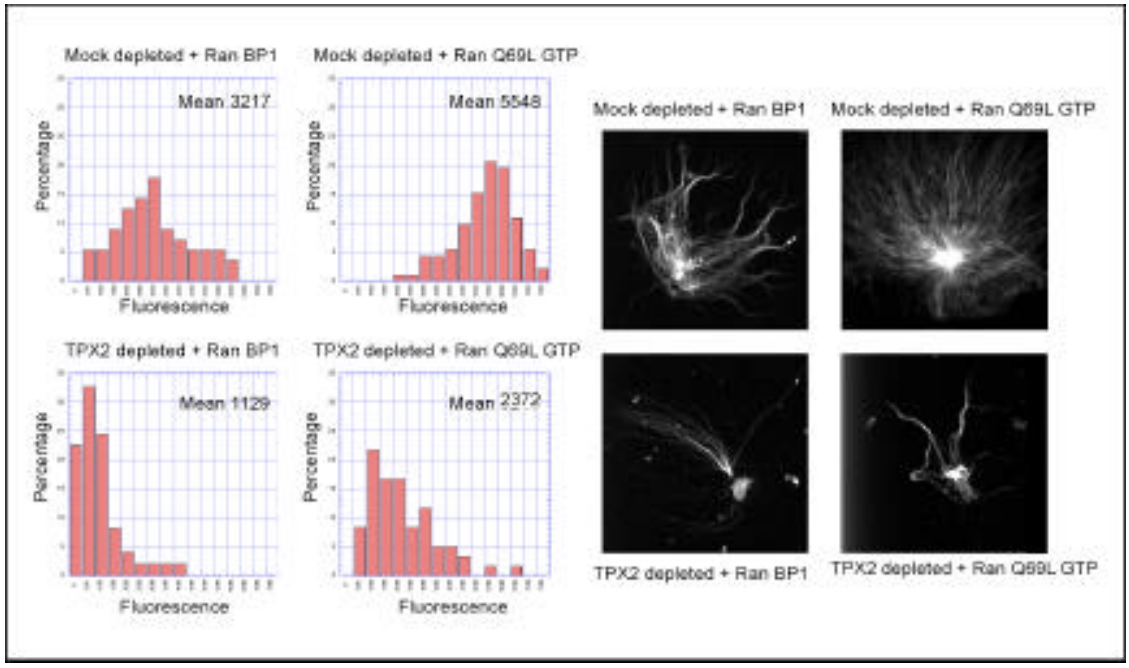

Figure 38. TPX2 is necessary for Ran dependent increase in microtubule nucleation by centrosomes.

Sperm centrosomes were incubated in *Xenopus* M phase extract either depleted of TPX2 or Mock depleted. Either 30 µM RanQ69LGTP or 10 µM RanBP1 and RanGAP were added. Quantification is based on total fluorescence as an indicator for microtubule mass. Y values give percentage of total asters with a particular fluorescence.

Ran impairs spindle formation in *Drosophila melanogaster*

Although highly conserved among vertebrate species, homologues of TPX2 or NuMA have not been found in other eukaryotes such as yeast, nematodes or *Drosophila.* However, experiments in *C. elegans* (Askjaer *et al*., 2002; Bamba *et al*., 2002) and yeast (Fleig *et al*., 2000) suggest that Ran may have a direct function in mitosis in all eukaryotes. To find out whether Ran affects microtubule organization in *Drosophila* we performed injection experiments. *Drosophila* embryogenesis begins with 13 metasynchronous mitotic cycles within a syncytial cytoplasm (Minden *et al*., 1989). These cycles consist only of S and M phases, rely on maternally supplied activities, and do not require zygotic gene expression.

Drosophila strains expressing either histone-H2B-GFP or GFP–αtubulin were provided by Cayetano González's laboratory. We injected syncytial stage embryos with different variants of Ran. Injection of ten percent the body volume of a 5 mg/ml protein solution of wild type Ran did not effect the embryos. On the other hand the same amount of RanQ69LGTP severely affected cell division and spindle formation (Figure 39). In the histone-H2B-GFP strain injected with RanQ69LGTP chromosome segregation close to the site of injection was dramatically slowed down and most nuclei are arrested in metaphase (Figure 39 upper row third panel from left). The GFP-tubulin strain was depleted of tubulin in the areas adjacent to the injection site, nuclei were not distributed equally and were sometimes bigger. Most striking was the appearance of very large microtubule asters in embryos injected with RanQ69LGTP (Figure 39).

Injection of Ran T24N also depleted tubulin close to the site of injection and cells did not divide anymore or showed tri or multipolar spindles (Figure 39). These experiments indicate that both mutant Ran variants affect cell division and microtubule organization in *Drosophila* syncytial embryos. On the other hand the interpretation of the observed phenotypes is difficult. The cell cycle stage in these embryos is not defined since the cells undergo a division every 9 minutes during the experiment. Ran is critical for nucleocytoplasmic transport, effects on microtubule organization can always be indirect due to mislocalization of proteins in interphase. A detailed analyses of mitotic functions of Ran in *Drosophila* awaits either an *in vitro* mitotic extract system or knowledge of functional homologues of TPX2 or NuMA in flies.

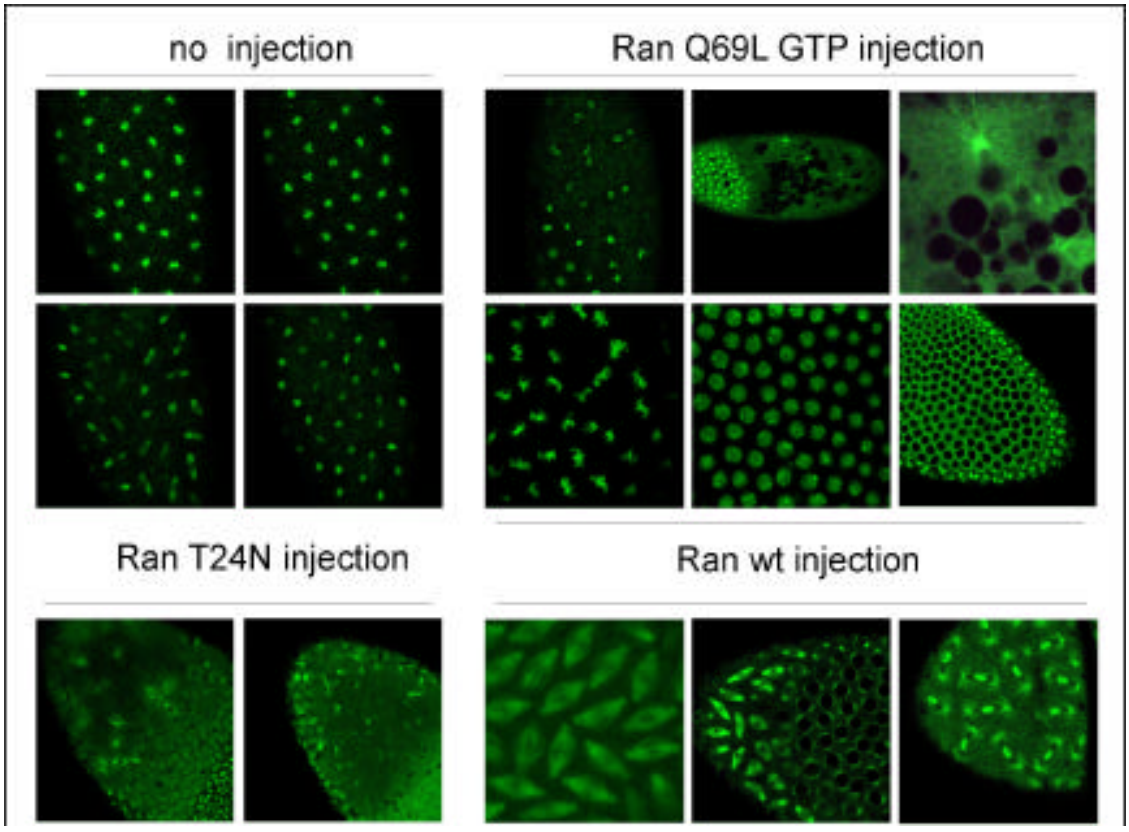

Figure 39. Ran effects spindle formation in *Drosophila* syncytial embryos

Syncytial stage *Drosophila* embryos expressing GFP-α-tubulin(upper right panels and panels at the bottom) or GFP-histone (upper left panels and panels in the middle) were injected with 1/10 volume of a protein solution containing 5 mg/ml of either Ran wild type (panels on the right middle and bottom), RanQ69LGTP (upper right panels) or Ran T24N (lower left panels).